Submitted to ADVANCED MATERIALS
DOI: 10.1002//adma.((please add manuscript number))

Radiation Hardness and Self-Healing of Perovskite Solar Cells

By *F. Lang*, N. H. Nickel, J. Bundesmann, S. Seidel, A. Denker, S. Albrecht, V. V. Brus, J. Rappich, B. Rech, G. Landi, and H. C. Neitzert*

[*] F. Lang, Prof. Dr. N. H. Nickel, Dr. S. Albrecht, Dr. V. V. Brus, Dr. J. Rappich, Prof. Dr. B. Rech
Helmholtz-Zentrum Berlin für Materialien und Energie GmbH, Institut für Silizium Photovoltaik, Kekuléstr. 5, 12489 Berlin, Germany.
E-mail: felix.lang@helmholtz-berlin.de

J. Bundesmann, S. Seidel, Dr. A. Denker
Helmholtz-Zentrum Berlin für Materialien und Energie GmbH, Protons for Therapy, Hahn-Meitner Platz 1, 14109 Berlin, Germany

Dr. G. Landi, Prof. Dr. H. C. Neitzert
Dept. of Industrial Engineering (DIIn), Salerno University, Via Giovanni Paolo II 132, 84084 Fisciano (SA), Italy

Keywords: perovskite solar cells, radiation hardness, proton irradiation, degradation, self-healing

Thin-film tandem solar cells, comprising of a perovskite top junction and a radiation hard CIGS bottom junction are attractive for space applications since they can be thin, lightweight, flexible, and efficient. The ability to withstand the harsh radiation environment in space, consisting mainly of high-energy protons is demonstrated. In-situ measurements of the $J - V$ characteristics during proton irradiation with an energy of 68 MeV reveal the stability of these novel organic-inorganic perovskites. The investigated $CH_3NH_3PbI_3$ based perovskite solar cells possess a negligible degradation for doses of up to 10^{12} p cm^{-2}. The observed degradation at very high doses is dominated by coloring of the glass substrate. Taking this effect and the photo-degradation into account the proton-induced absorber degradation shows a change of J_{SC} by only 20 % at a proton dose of 10^{13} p cm^{-2}, while the open circuit voltage remains constant. In addition to the superior radiation hardness, $CH_3NH_3PbI_3$ exhibits a self-healing mechanism when the proton irradiation is terminated. The photocurrent and the photovoltaic performance of the perovskite recover with time.

1. Introduction

Solar cells based on hybrid perovskites, such as methyl ammonium lead iodide ($CH_3NH_3PbI_3$), showed already excellent device performances with efficiencies exceeding 20 %[1] after an impressive short research and development time.[1,2] Band-gap tuning over a wide energy range [3–5] makes this class of materials interesting for multi-junction solar cells with ultra-high efficiencies. Tandem solar-cells combining perovskites with Si[5–11], $Cu(In,Ga)Se_2$[9,12,13], and $Cu_2ZnSn(S,Se)_4$[14]have been reported. Such high power multi-junction solar cells are needed for spaceships and satellites in outer space, where efficiency, size, and weight represent important factors. On the other hand, ionizing radiation, mainly helium (He) and protons (p), originating from either galactic cosmic radiation or solar flares is known to affect electronic devices by defect creation. [15] Depending on exposition and distance from earth the particle flux varies between 10^3 and 10^8 particles cm^{-2} s^{-1}.[16–19] Hence, a dose of 10^{13} particles cm^{-2} can be reached in about one day. This has been shown to have a tremendous effect on the power conversion efficiency of silicon, InGaP, GaAs, and InP solar cells that are commonly used in space. [20] For example, the Equator-S Mission, equipped with an GaAs/Ge solar cell reported a reduction in efficiency of around 10 % after 30 days in the low earth orbit.[21] Interestingly, one of the most radiation resistant solar-cell absorber materials, namely, copper indium gallium di-selenide (CIGS)[20] is rarely used due to its moderate power-conversion efficiency.[22] A thin-film tandem solar cell comprising of a CIGS bottom- and a perovskite top junction seems to be an ideal candidate to overcome this limitation. In principle, the combination should allow a new generation of efficient, lightweight, thin, and flexible solar-cell arrays for space applications. Solar-cell array foils that self-enfold once launched into orbit are imaginable.[23] Moreover, it is conceivable that radiation resistant devices based on hybrid perovskites are employed in harsh environments like damaged nuclear power plants. However, before such revolutionary designs will be

implemented, the radiation resistance of these organic-inorganic perovskites has to be demonstrated. Therefore, we present a study on the radiation hardness of $CH_3NH_3PbI_3$ using 68 MeV proton irradiation. *In-situ* measurements revealed a superior radiation resistance in comparison to a commercially available crystalline silicon (c-Si) photo-diode. In light of the reported instabilities of perovskite solar cells, the observed radiation resistance is remarkable.[24]

2. Results and Discussion

Proton-induced defect creation occurs due to ionization and lattice displacement effects. In addition, proton irradiation can also stimulate nuclear reactions due to proton capture of atoms. Typically, the newly generated nuclei are radioactive. Therefore, after the radiation experiments the samples must remain in the radiation safety controlled area delaying device characterization of the sensitive perovskites. In order to investigate the radiation hardness of the hybrid perovskite $CH_3NH_3PbI_3$, we decided to track the development of the short circuit current, J_{SC}, the open circuit voltage, V_{OC}, the fill factor, *FF*, and the power conversion efficiency, η, *in-situ* under illumination during irradiation with protons. Hence, the $J - V$ characteristics of 6 devices were measured simultaneously every 30 seconds. Three of these devices were exposed to proton irradiation, while the remaining solar cells served as a reference. Proper encapsulation of the solar cells allowed taking additional measurements after the radioactivity decreased to a safe level.

2.1. Solar Cell Performance

Typical perovskite solar cells based on TiO_2 and spiro-OMeTAD show pronounced hysteresis effects. [25–27] This would complicate the correct analysis of the *in-situ*

measurements during proton irradiation. Therefore, we chose the inverted staggered structure with a layer sequence of glass/ITO/PEDOT:PSS/$CH_3NH_3PbI_3$/PCBM/BCP/Ag. This structure has the advantage that a hysteresis of the $J - V$ characteristics is negligible. [26] Fig. 1(b) shows a simplified sketch of the used device structure and a cross-sectional scanning electron microscopy (SEM) micrograph is depicted in Fig 1(a). The film homogeneity is controlled by using a mixture of the solvents γ-butryolactone (GBL) / dimethyl sulfoxide (DMSO) and by a toluene dripping in a late spin coating stage. [28] Details on the device preparation are given in the experimental section.

Figure 1(d) shows the current-voltage characteristics of as-fabricated solar cells under AM 1.5G illumination. Due to the used inverted structure a hysteresis in the $J - V$ curves is negligible. The power conversion efficiency derived from the $J - V$ curve amounted to η = 12.1 % [see Fig. 1(d)]. This is corroborated by measuring the power conversion efficiency as a function of time using a maximum power-point tracking algorithm [inset in Fig. 1(d)]. After 400 s a stabilized value of η = 12.1 % was obtained. The fill factor, open circuit voltage, and short circuit current amounted to FF = 71 %, V_{OC} = 0.95 V, and J_{SC} = 17.9 mA/cm^2, respectively. Because of their high performance, stability, and lack of hysteresis effects the solar cells employed in this study are well suited to investigate degradation effects related to the absorber radiation hardness. The external (EQE) and internal quantum efficiencies (IQE) are depicted in Fig. 1(e). The integrated short circuit current amounts to 17.4 mAcm^{-2} and matches the value obtained under AM1.5 illumination.

2.2 Radiation Hardness under Proton Irradiation

Ionizing radiation in space is dominated by high energy protons in the MeV range[29,30]. In particular, protons with energies close to 1 MeV have a high stopping cross-section and therefore, can cause severe damage to electronic devices and solar cells.[31] On the other hand,

an effective radiation guard requires only a view millimeters of shielding. Thus, for our study we have chosen a proton energy of 68 MeV that still causes considerable damage while having a projected range of several centimeters. This ensures homogeneous defect creation throughout the entire perovskite absorber. The proton energy-loss is shown in Fig. 1(c) as a function of the target depth. The data were derived from a SRIM calculation.[32]

Three identical perovskite solar cells were exposed to proton irradiation with a total proton dose of $\phi = 1.02\times10^{13}$ p cm^{-2}. The experiments were performed at the cyclotron facility of the Helmholtz-Zentrum Berlin. [33,34] The proton flux was kept constant at about $\varphi = 1.68\times10^{9}$ p cm^{-2} s^{-1}. The total dose of 1.02×10^{13} p cm^{-2} was accumulated after 101 min. Fig. 2 shows the degradation of the photovoltaic parameters J_{SC}, V_{OC}, and η of an irradiated device as a function of the proton dose, ϕ.

Upon proton irradiation J_{SC} and the power conversion efficiency, η, decrease (red and open circles in Fig. 2(a)), while the open circuit voltage and the fill factor remain constant (blue diamonds and black triangles in Fig. 2(a)). Hence, the proton-induced decrease of η is solely caused by a decrease of J_{SC}, which changes due to the generation of localized defects. It is important to note that the perovskite solar cells do not exhibit any degradation for a proton dose of $\phi \leq 2\times10^{11}$ p cm^{-2}. Only at higher proton doses a decrease of J_{SC} and η is observed with a reduction of around 10 % and 40 % for $\phi = 10^{12}$ p cm^{-2} and 10^{13} p cm^{-2}, respectively. On the other hand, the impact of proton-irradiation experiments on the short-circuit current of a commercially available c-Si photo diode shows pronounced degradation due to defect creation even for a low proton dose. A 40 % decrease of the photo current is observed for a proton dose of only $\phi = 7\times10^{11}$ p cm^{-2} (blue curve in Fig. 2(a)). This is in good agreement with previous reports for c-Si solar cells.[35] The data shown in Fig. 2(a) clearly demonstrate that perovskite solar cells are significantly less affected by proton radiation than c-Si devices.

In addition to the degradation of the absorber layer, proton irradiation can affect other layers in a solar cell. An example is the creation of color centers in the glass substrate.[36,37] As a result some light will be absorbed in the glass and consequently, the performance of the solar cell decreases. Fig. 2 (b) shows the transmission spectra of ITO coated glass substrates before (black curve) and after proton irradiation (blue and red curves). The coloring of the glass affects the transmission spectra in the spectral range between 300 and 800 nm. This shading effect is depicted by the hatched areas in Fig. 2 (b). As a remark, optical glasses can be stabilized against radiation induced coloring for example by adding lanthanum or cerium.[36]

Since *in-situ* measurements of the solar cells were performed during proton irradiation the formation of color centers in the substrate has to be taken into account. The data shown in Fig. 2(b) were used to separate the degradation of the perovskite layer due to proton irradiation from the formation of color centers in the glass substrate. For a proton dose of 10^{13} p cm^{-2} a decrease of J_{SC} of about 20 % is observed. This is shown by the red diamond in Fig. 2 (a). Hence, the perovskite layers can withstand proton doses as high as 10^{12} p cm^{-2} before degradation commences. This exceeds the proton dose at which c-Si begins to degrade by almost 3 orders of magnitude. Thus, we have experimentally demonstrated that the perovskite layers are radiation hard making them a desirable material in solar cells for space applications.

2.3 Self-healing

The *in-situ* measurements of the perovskite solar cells were continued after the proton irradiation was terminated. In Fig. 3 the time dependence of the normalized short-circuit current, open circuit voltage, fill factor, and power conversion efficiency are shown for the

sample irradiated with a proton dose of $\phi = 1\times10^{13}$ p cm^{-2} (red circles) and a reference sample that was *not* exposed to high-energy protons (black diamonds). Here, $t - t_{irr} = 0$ s corresponds to the end of the irradiation experiment. Surprisingly, J_{SC} and η of the proton-irradiated device increase continuously with time, while V_{OC} and the fill factor remain constant. A change of J_{SC} is mainly due to a change in the concentration of localized defects. Hence, this result shows that the perovskite solar cells possess a self-healing capability that lowers the number of defects caused by proton irradiation. It is likely that proton-induced defect creation and self-healing is due to ion and/or atom displacements. It is important to note that self-healing occurs at room temperature. Hence, the migration barrier for atoms and ions is expected to be small. This is consistent with the low crystallization temperature of the perovskites.

Proton irradiation experiments produce radioactive elements in the exposed materials that decay to a tolerable level within about 10 days. After this waiting period the irradiated solar cells and the reference devices were characterized again. It is important to note that the reference devices were exposed to the same photon flux as the proton irradiated solar cells and were also kept in the radiation cabinet for 10 days. The photovoltaic parameters of three proton and three reference solar cells are plotted in Fig. 4 (a). Due to the prolonged illumination with an AM1.5G spectrum all parameters of the reference solar cells degraded and an average efficiency of $\eta \approx 5.7$ % was obtained (black diamonds in Fig. 4). The proton-irradiated solar cells show a more pronounced decrease of J_{SC} while the open circuit voltage and the fill factor increased, which resulted in about the same efficiency of $\eta \approx 5.7$ % (full red circles in Fig. 4). However, for the proton-irradiated specimens the formation of color centers in the glass substrate has to be taken into account. When correcting for this deleterious effect J_{SC} increases to about 11.7 mAcm^{-2}. Interestingly, this results in a higher power conversion efficiency of $\eta \approx 8.0$ % compared to the reference devices (open red circles in Fig. 4 (a)). The

internal quantum efficiency (IQE) and the reflection of a reference and a proton-irradiated solar cell are plotted in Fig. 4(b). The change of the integrated IQE curve due to proton-irradiation corresponds to the observed decrease of J_{SC} (Fig. 4(a)).

Proton irradiation has detrimental consequences for the host material. Besides the production of impurities through transmutation of nuclei that may be radioactive, atom displacement may occur through the transfer of kinetic energy. When atoms are displaced from their lattice site vacancies and an interstitials are created. These Frenkel pairs [38] can cause secondary displacements. Recently, it was speculated that ion migration might be responsible for instabilities observed in perovskites.[39] In particular, changes of the photoluminescence with time in $CH_3NH_3PbI_3$ were attributed to the migration of iodine.[40] Furthermore, charged particles like protons directly ionize the host lattice. In general, ionizing radiation damages the host material by disrupting bonds between atoms. Most susceptible are covalent bonds since their energies are in the low eV range.[41] Hence, the following picture is conceivable. Proton irradiation causes significant ionization of the perovskite lattice that eventually leads to the dissociation of ionic and covalent bonds. Since covalent bonds are more susceptible than ionic bonds[41] most radiation-induced damage may occur at the organic CH_3-NH_3 molecules by the breaking of C-H, C-N, and/or N-H bonds. In organic semiconductors the dissociation of C-H bonds upon irradiation is well-known.[40,41] In fact, it has been shown that the release of H atoms causes the formation of localized defect-states in the bandgap that act as recombination centers.[43] Hence, it is likely that proton irradiation results in the dissociation of C-H and N-H bonds giving rise to localized states in the bandgap of the perovskite. This picture is consistent with results from electron spin resonance experiments in combination with calculations which showed that fragmented methyl-ammonium gives rise to localized defects in the bandgap of perovskites.[44] When the proton irradiation is terminated the solar cells exhibit a self-healing mechanism. It is conceivable that displaced hydrogen atoms migrate in the perovskite lattice and passivate both, newly

generated localized defects due to the proton irradiation and pre-existing defects. Consequently, this leads to an improvement of the proton irradiated solar cells when compared to the reference devices.

3. Summary

In summary, we have fabricated inverted perovskite solar cells with a layer sequence of glass/ITO/PEDOT:PSS/$CH_3NH_3PbI_3$/PCBM/BCP/Ag. The inverted structure is beneficial for *in-situ* proton irradiation experiments since it does not suffer from a hysteresis effect in the $J - V$ characteristics. The solar cells had a stabilized power conversion efficiency of η = 12.1 %. The devices were irradiated with 68 MeV protons until a total dose of 1.02×10^{13} p cm^{-2} was reached. During the irradiation experiments $J - V$ curves were measured every 30 s. A decrease of J_{SC} by 10 % and 40 % was observed for a proton dose of $\phi = 10^{12}$ p cm^{-2} and 10^{13} p cm^{-2}, respectively. However, when the data are corrected for deleterious effects, such as the photo degradation of the perovskite layer as measured on a reference, the decrease of J_{SC} amounts to only 20 %. A degradation of V_{OC} and the fill factor is not observed. Hence, the perovskite absorber can withstand proton doses up to 10^{12} p cm^{-2}, which exceeds the damage threshold of c-Si by almost 3 orders of magnitude. Moreover, when the proton irradiation is terminated a self-healing process of the perovskite commences and J_{SC} recovers. After 10 days V_{OC} and the fill factor were significantly enhanced compared to the reference devices. The fact that $CH_3NH_3PbI_3$ perovskites are radiation hard and exhibit self-healing renders these solar cells highly attractive for space applications.

4. Experimental

Preparation of Perovskite Solar Cells: Planar inverted perovskite solar cells were prepared with the layer sequence glass/ITO/PEDOT:PSS/$CH_3NH_3PbI_3$/$PC_{61}BM$/BCP/Ag. First, the ITO coated glass substrates were cleaned using acetone, detergent/H_2O, H_2O, isopropanol, and O_3. Then, a 60 nm thick PEDOT:PSS layer was deposited by spin-coating at 3000 rpm for 30 s. Subsequently, the PEDOT:PSS layer was annealed at 150 °C for 20 min.

A stoichiometric $CH_3NH_3PbI_3$ precursor solution containing 1.1 M of PbI_2 and CH_3NH_3I was prepared in a mixed solvent of γ-butryolactone and dimethyl sulfoxide with a volume ratio of 70 vol.% to 30 vol.%. The solution was stirred for 12 h at 60°C. In a second step, the $CH_3NH_3PbI_3$ solution was spin coated with the following sequence: 1000 rpm for 10 s, 2000 rpm for 20 s, and 5000 rpm for 20 s. At the last stage 150 µl toluene were dripped on top of the $CH_3NH_3PbI_3$ layer [28]. Spin coating was performed in nitrogen atmosphere. Subsequently, the $CH_3NH_3PbI_3$ layer was crystallized at 100 °C for 10 min. The absorber had a thickness of d = 350 nm. The electron selective contact was formed by spin coating a ~50 nm thick $PC_{61}BM$ layer at 2500 rpm for 60 s. After annealing for 10 min at 100 ºC a thin layer of bathocuproine (BCP) was spin coated from ethanol solution (0.5 mg/ml, 4000 rpm, 45 s). Subsequently, the devices were annealed at 70°C for 15 min and transferred into an evaporation chamber with a base pressure of about 10^{-7} mbar. Electrical contacts consisting of 100 nm Ag were thermally evaporated using a shadow mask. The overlap of the patterned ITO and the metal contacts defined the active area of the solar cells and amounted to 0.16 cm^2.

Characterization: The perovskite solar cells were characterized using an AM1.5G simulated solar spectrum. Because of the well-known hysteresis effect [25,27] current-voltage scans were performed in forward and reverse direction using a voltage sweep of 85 mV/s. For the inverted solar cell structures, a hysteresis was not observed and the maximum power points for forward and reverse scan directions were identical. The external quantum efficiency was measured without bias voltage and illumination. Prior to the characterization the solar

cells were light soaked for 30 min. The proton irradiation experiments were performed at the cyclotron of the Helmholtz-Zentrum Berlin. [33,34] The proton energy was 68 MeV. The Tandetron-cyclotron combination provides a high stability of the beam intensity. To achieve a homogeneous irradiation over an area of 3.0 cm^2 wobbler magnets were used. The beam intensity was monitored online using a transmission ionization chamber. During proton irradiation *in-situ* measurements were performed using a halogen lamp. The light intensity was about 25 mW/cm^2. A crystalline silicon photo-diode 'BPW34' purchased from Vishay semiconductors was used as reference.

Acknowledgements

The authors are grateful to C. Klimm for taking SEM micrographs. Financial support from the Seventh Framework Program of the European Union under grant No. 604032 is acknowledged. V. V. Brus acknowledges the Alexander-von-Humboldt foundation for financial support.

Figures

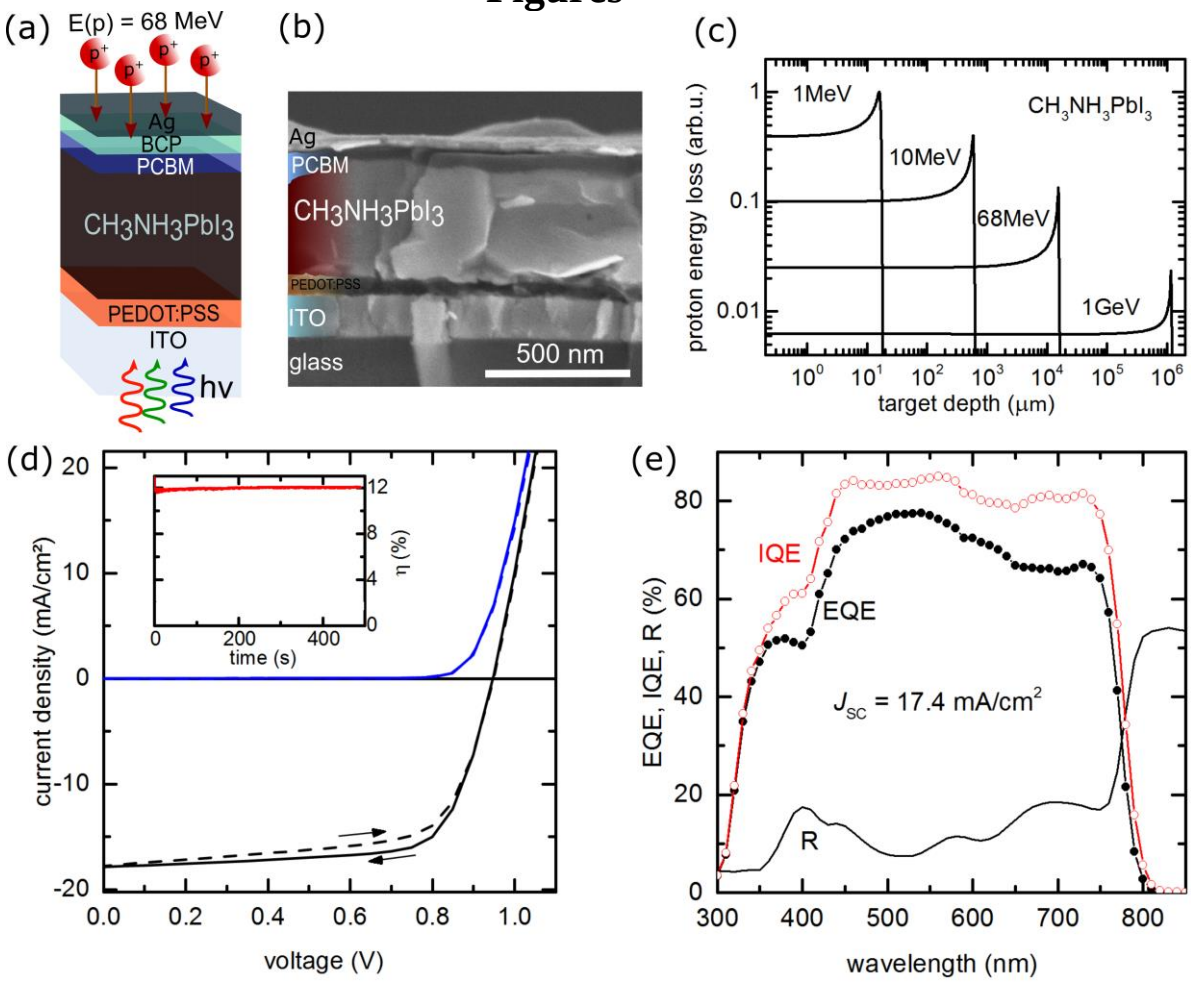

Fig. 1. (a) Cross-sectional SEM micrograph of an inverted staggered perovskite solar cell consisting of the layer stack glass/ITO/PEDOT:PSS/$CH_3NH_3PbI_3$/PCBM/BCP/Ag. (b) shows a sketch of the perovskite solar cell. Proton irradiation was performed through the Ag electrode while the device was illuminated through the glass substrate. The projected range of the proton beam in the perovskite $CH_3NH_3PbI_3$ is shown in (c). The simulation was performed using SRIM [32]. (d) shows current-voltage characteristics of the perovskite solar cell taken prior to the proton irradiation. The blue curve was measured in the dark and the black curves were taken under AM1.5G illumination. The scan direction of the voltage is indicated by arrows. A hysteresis between reverse scan (solid line) and forward scan (dashed line) is negligible. The inset shows the stabilized efficiency from maximum power point tracking. (e)

Shows the external (EQE) and internal (IQE) quantum efficiencies. The black solid line depicts the specular reflection.

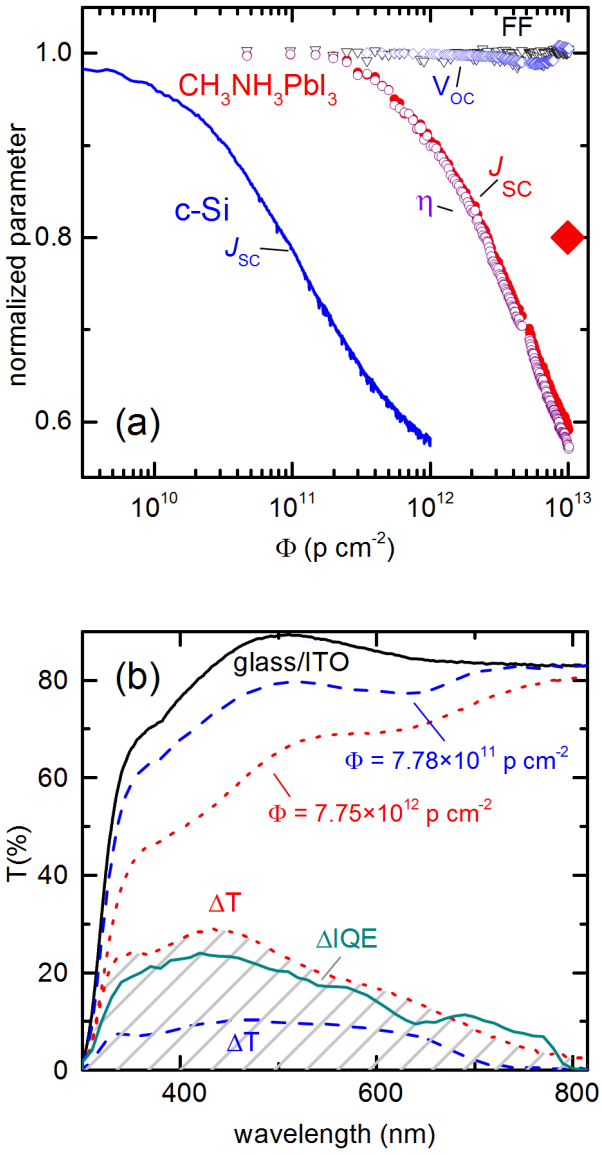

Fig. 2. (a) Normalized solar cell parameters as a function of the proton dose, ϕ. Symbols depict the evolution of the short-circuit current J_{SC}, the fill factor FF, the efficiency η, and the open circuit voltage V_{OC} of a perovskite solar cell. The red diamond depicts the normalized value of J_{SC} at the end of the proton irradiation experiment after correcting for transmission losses due to color centers in the substrate. The blue curve shows the evolution of the J_{SC} of a c-Si photo-diode. (b) Diffuse transmission of glass/ITO substrates before (black solid curve) and after proton irradiation with a dose of $\phi = 7.78\times10^{11}$ p cm^{-2} (blue dashed curve) and $\phi =$

7.75×10^{12} p cm^{-2} (red dotted line). The resulting shading (ΔT) is shown by hatched red and blue curves. The difference of the internal quantum efficiencies (ΔIQE) from Fig 4 (b) is shown by the solid green line.

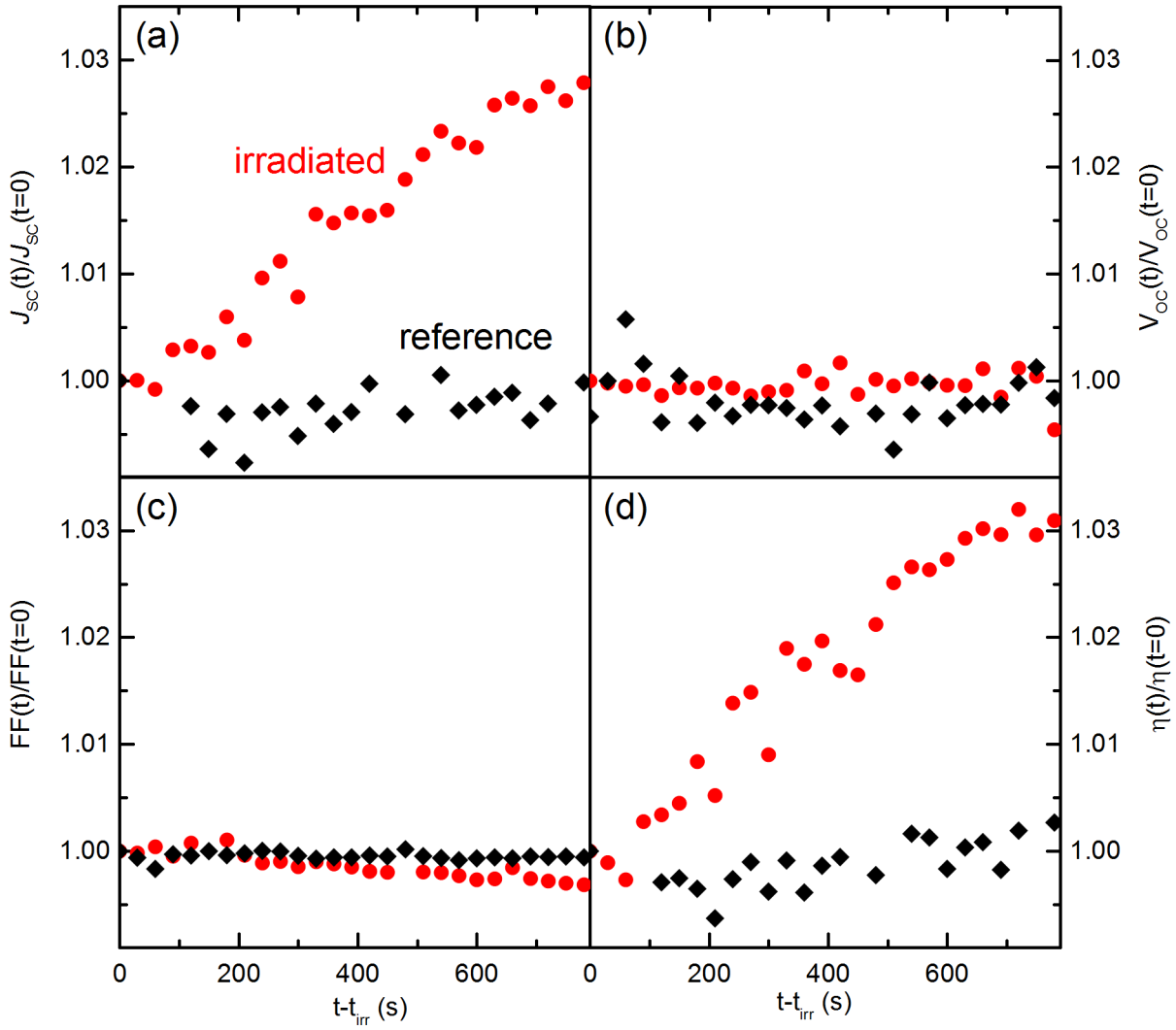

Fig. 3. Time dependence of the normalized solar-cell parameters after termination of the proton irradiation for a proton irradiated device (red circles) and for a reference solar cell (black diamonds). The data are normalized to unity at $t - t_{irr} = 0$.

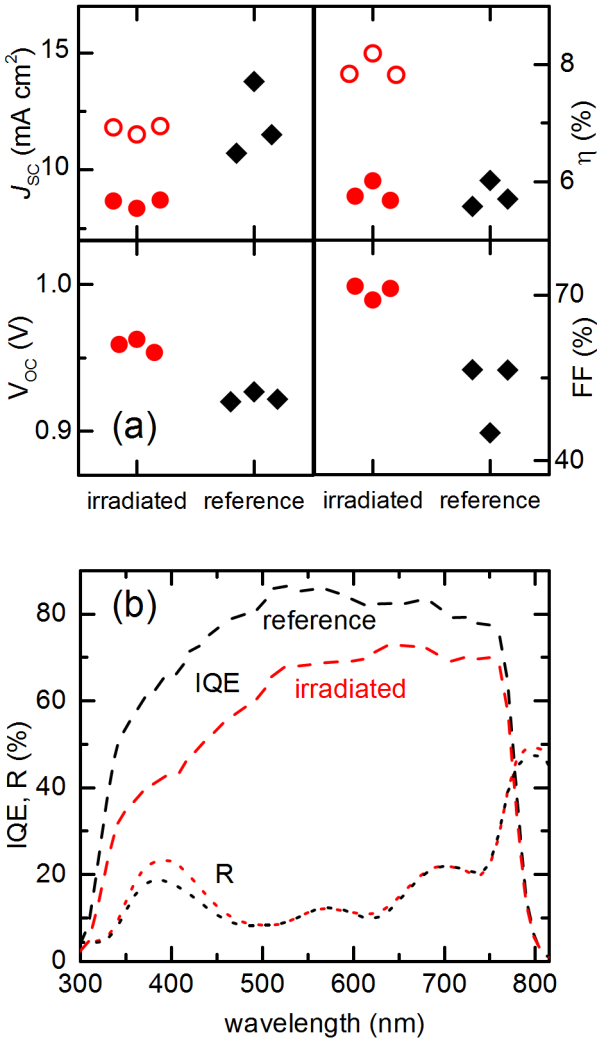

Fig. 4. (a) comparison of the photovoltaic parameters of irradiated perovskite solar cells and reference devices under AM1.5G. The data (full symbols) were measured after the radioactivity decayed to a tolerable level within 10 days. The open circles represent the short circuit current and the efficiency of the proton irradiated solar cells taking the formation of color centers in the substrates into account. (b) shows the internal quantum efficiency (IQE) and reflection (R) of the reference (black) and the proton irradiated device (red).

Reference:

[1] W. S. Yang, J. H. Noh, N. J. Jeon, Y. C. Kim, S. Ryu, J. Seo, S. I. Seok, *Science* **2015**, *348*, 1234.

[2] H. J. Snaith, *J. Phys. Chem. Lett.* **2013**, *4*, 3623.

[3] J. H. Noh, S. H. Im, J. H. Heo, T. N. Mandal, S. Il Seok, *Nano Lett.* **2013**, *13*, 1764.

[4] M. R. Filip, G. E. Eperon, H. J. Snaith, F. Giustino, *Nat. Commun.* **2014**, *5*, 5757.

[5] D. P. McMeekin, G. Sadoughi, W. Rehman, G. E. Eperon, M. Saliba, M. T. Horantner, A. Haghighirad, N. Sakai, L. Korte, B. Rech, M. B. Johnston, L. M. Herz, H. J. Snaith, *Science* **2016**, *351*, 151.

[6] F. Lang, M. A. Gluba, S. Albrecht, J. Rappich, L. Korte, B. Rech, N. H. Nickel, *J. Phys. Chem. Lett.* **2015**, *6*, 2745.

[7] S. Albrecht, M. Saliba, J. P. Correa Baena, F. Lang, L. Kegelmann, M. Mews, L. Steier, A. Abate, J. Rappich, L. Korte, R. Schlatmann, M. K. Nazeeruddin, A. Hagfeldt, M. Grätzel, B. Rech, *Energy Environ. Sci.* **2016**, *9*, 81.

[8] P. Löper, S.-J. Moon, S. Martín de Nicolas, B. Niesen, M. Ledinsky, S. Nicolay, J. Bailat, J.-H. Yum, S. De Wolf, C. Ballif, *Phys. Chem. Chem. Phys.* **2015**, *17*, 1619.

[9] L. Kranz, A. Abate, T. Feurer, F. Fu, E. Avancini, J. Löckinger, P. Reinhard, S. M. Zakeeruddin, M. Grätzel, S. Buecheler, A. N. Tiwari, *J. Phys. Chem. Lett.* **2015**, *6*, 2676.

[10] R. Sheng, A. W. Y. Ho-Baillie, S. Huang, M. Keevers, X. Hao, L. Jiang, Y.-B. Cheng, M. A. Green, *J. Phys. Chem. Lett.* **2015**, *6*, 3931.

[11] J. Werner, G. Dubuis, A. Walter, P. Löper, S.-J. Moon, S. Nicolay, M. Morales-Masis,

S. De Wolf, B. Niesen, C. Ballif, *Sol. Energy Mater. Sol. Cells* **2015**, *141*, 407.

[12] C. D. Bailie, M. G. Christoforo, J. P. Mailoa, A. R. Bowring, E. L. Unger, W. H. Nguyen, J. Burschka, N. Pellet, J. Z. Lee, M. Grätzel, R. Noufi, T. Buonassisi, A. Salleo, M. D. McGehee, *Energy Environ. Sci.* **2014**, *8*, 956.

[13] F. Fu, T. Feurer, T. Jäger, E. Avancini, B. Bissig, S. Yoon, S. Buecheler, A. N. Tiwari, *Nat. Commun.* **2015**, *6*, 8932.

[14] T. Todorov, T. Gershon, O. Gunawan, C. Sturdevant, S. Guha, *Appl. Phys. Lett.* **2014**, *105*.

[15] B. Todd, S. Uznanski, *CAS - Cern Accel. Sch. Power Convert.* **2015**, *003*, 1.

[16] R. Schwenn, In *The Encyclopedia of Astronomy and Astrophysics*; IOP Publishing Ltd, 2001; pp. 1–9.

[17] D. Mottl, R. Nymmik, *Adv. Space Res.* **2003**, *32*, 2349.

[18] T. Markvart, *J. Mater. Sci. Mater. Electron.* **1990**, *1*, 1.

[19] E. J. Daly, G. Drolshagen, A. Hilgers, H. D. R. Evans, *Space Environment Analysis: Experience and Trends*.

[20] A. Jasenek, U. Rau, K. Weinert, H. W. Schock, J. H. Werner, *Photovolt. Energy Conversion, 2003. Proc. 3rd World Conf.* **2003**, *1*, 593.

[21] S. R. Messenger, G. P. Summers, E. A. Burke, R. J. Walters, M. A. Xapsos, *Prog. Photovoltaics Res. Appl.* **2001**, *9*, 103.

[22] P. Iles, *Sol. Energy Mater. Sol. Cells* **2001**, *68*, 1.

[23] A. Kumar, R. Devine, C. Mayberry, B. Lei, G. Li, Yang, *Adv. Funct. Mater.* **2010**, *20*, 2729.

[24] X. Zhao, N.-G. Park, *Photonics* **2015**, *2*, 1139.

[25] H. J. Snaith, A. Abate, J. M. Ball, G. E. Eperon, T. Leijtens, N. K. Noel, S. D. Stranks, J. T.-W. Wang, K. Wojciechowski, W. Zhang, *J. Phys. Chem. Lett.* **2014**, *5*, 1511.

[26] H.-S. Kim, I.-H. Jang, N. Ahn, M. Choi, A. Guerrero, J. Bisquert, N.-G. Park, *J. Phys.*

Chem. Lett. **2015**, *6*, 4633.

[27] E. L. Unger, E. T. Hoke, C. D. Bailie, W. H. Nguyen, A. R. Bowring, T. Heumuller, M. G. Christoforo, M. D. McGehee, *Energy Environ. Sci.* **2014**, *7*, 3690.

[28] N. J. Jeon, J. H. Noh, Y. C. Kim, W. S. Yang, S. Ryu, S. Il Seok, *Nat. Mater.* **2014**, *13*, 897.

[29] G. D. Badhwar, P. M. O'Neill, *Int. J. Radiat. Appl. Instrumentation. Part D. Nucl. Tracks Radiat. Meas.* **1992**, *20*, 403.

[30] G. D. Badhwar, P. M. O'Neill, *Adv. Space Res.* **1996**, *17*, 7.

[31] H. C. Neitzert, P. Spinillo, S. Bellone, G. D. Licciardi, M. Tucci, F. Roca, L. Gialanella, M. Romano, *Sol. Energy Mater. Sol. Cells* **2004**, *83*, 435.

[32] J. F. Ziegler, M. D. Ziegler, J. P. Biersack, *Nucl. Instruments Methods Phys. Res. Sect. B Beam Interact. with Mater. Atoms* **2010**, *268*, 1818.

[33] A. Denker, C. Rethfeldt, J. Röhrich, H. Berlin, D. Cordini, J. Heufelder, R. Stark, A. Weber, B. H. Berlin, *Proc. CYCLOTRONS 2010, (Lanzhou, China)* **2010**, 75.

[34] J. Röhrich, T. Damerow, W. Hahn, U. Müller, U. Reinholz, A. Denker, *Rev. Sci. Instrum.* **2012**, *83*, 02B903.

[35] H.-C. Neitzert, M. Ferrara, M. Kunst, A. Denker, Z. Kertész, B. Limata, L. Gialanella, M. Romano, *Phys. status solidi B* **2008**, *245*, 1877.

[36] A. I. Gusarov, D. Doyle, A. Hermanne, F. Berghmans, M. Fruit, G. Ulbrich, M. Blondel, *Appl. Opt.* **2002**, *41*, 678.

[37] M. F. Bartusiak, J. Becher, *Appl. Opt.* **1979**, *18*, 3342.

[38] J. Frenkel, *Zeitschrift für Phys.* **1926**, *35*, 652.

[39] Y. Yuan, J. Huang, *Acc. Chem. Res.* **2016**, *49*, 286.

[40] D. W. deQuilettes, W. Zhang, V. M. Burlakov, D. J. Graham, T. Leijtens, A. Osherov, V. Bulović, H. J. Snaith, D. S. Ginger, S. D. Stranks, *Nat. Commun.* **2016**, *7*, 11683.

[41] R. A. Knief, *Nuclear Energy Technology*; McGraw-Hill, 1981.

[42] F. Bebensee, J. Zhu, J. H. Baricuatro, J. A. Farmer, Y. Bai, H. P. Steinrück, C. T. Campbell, J. M. Gottfried, *Langmuir* **2010**, *26*, 9632.

[43] R. A. Street, J. E. Northrup, B. S. Krusor, *Phys. Rev. B - Condens. Matter Mater. Phys.* **2012**, *85*, 1.

[44] P. Delugas, A. Filippetti, A. Mattoni, *Phys. Rev. B - Condens. Matter Mater. Phys.* **2015**, *92*, 1.

The radiation hardness of $CH_3NH_3PbI_3$ based solar cells is evaluated from *in-situ* measurements during high-energy proton irradiation. These organic-inorganic perovskites exhibit radiation hardness and withstand proton doses that exceed the damage threshold of c-Si by almost 3 orders of magnitude. Moreover, after termination of the proton irradiation a self-healing process of the solar cells commences. Radiation hardness and self-healing renders these solar cells highly attractive for space applications.

ToC figure: